Anisotropic optical response of the diamond (111)-2×1 surface

Cecilia Noguez

Instituto de Física, Universidad Nacional Autónoma de México, Apartado Postal 20-364, México Distrito Federal 01000, Mexico

Sergio E. Ulloa

Department of Physics and Astronomy, and Condensed Matter and Surface Science Program,
Ohio University, Athens, Ohio 45701-2979
(Received 27 November 1995)

The optical properties of the 2×1 reconstruction of the diamond (111) surface are investigated. The electronic structure and optical properties of the surface are studied using a microscopic tight-binding approach. We calculate the dielectric response describing the surface region and investigate the origin of the electronic transitions involving surface and bulk states. A large anisotropy in the surface dielectric response appears as a consequence of the asymmetric reconstruction on the surface plane, which gives rise to the zigzag Pandey chains. The results are presented in terms of the reflectance anisotropy and electron energy loss spectra. While our results are in good agreement with available experimental data, additional experiments are proposed in order to unambiguously determine the surface electronic structure of this interesting surface.

I. INTRODUCTION

Apart from being of fundamental interest, the characterization of the low-index diamond surface is very important from a technological point of view. The fast development of chemical vapor deposition techniques has increased the demand for a better understanding of the ground state and excited properties of these surfaces.[1] Indeed, much experimental and theoretical attention has been paid to the characterization of the geometrical structure, vibrational modes, and electronic properties of these surfaces, with interesting and sometimes controversial results. In this work, we are interested in characterizing the *optical* response of the (111) diamond surface, and investigating how these properties are related to the structural reconstruction and its accompanying electronic structure.

Our interest in this particular surface includes concerns on discrepancies between the present experimental[2–7] and theoretical results.[8–11] Experimentally, a great deal of the surface electronic structure is well known through angle resolved photoemission spectroscopy (ARPES),[2,3] soft-x-ray absorption,[6] inverse photoemission,[7] and electron energy loss spectroscopy (EELS).[4,5] The photon-induced measurements show a variety of occupied[2,3] and unoccupied[6,7] surface states lying in the fundamental gap. However, the complete description of these surface states has been difficult, since their dispersion along only a few of the main directions of the surface unit cell has been measured. On the other hand, EELS measurements[4] show a prominent broad feature at about 2.1 eV, which is attributed to transitions from occupied to unoccupied surface states. Since EELS experiments measure a transition energy which is generally smaller than the difference between occupied and unoccupied states, and a relatively large uncertainty (± 0.6 eV) accompanied this particular EELS experiment, a direct comparison with other results has not been possible.

Several theoretical studies have been done to elucidate the structural and electronic properties of the C(111)-2×1 surface. Both *ab initio*[8–10] and semiempirical[11] theoretical approaches have been employed, yielding some differences among them and with experimental results. Some of these differences arise from the methodology employed. For example, Iarlori and co-workers[9] employed a local-density approximation (LDA) formalism using a plane wave basis, while Vanderbilt and Louie[8] and Alfonso and co-workers[10] used the LDA formalism based on a set of localized orbitals. In the former work the energy gaps are underestimated,[9] as is common in this kind of approximation, and a direct comparison to experimental results is difficult. The latter theoretical works compare well among them,[8,10] although a systematic shift of about 1 eV is found when the surface states are compared with those measured experimentally.[2,3,6,7] On the other hand, the semiempirical tight-binding approach of Davidson and Pickett[11] compares well with the *ab initio* results described above, except for an extra shift of the surface states by about 0.8 eV. Since the surface states determine the location of the Fermi level, there is a large discrepancy among different theoretical works as to the relative position of the Fermi level and the top of the valence band that goes from -1.3 to 2 eV. On the other hand, in all theoretical and experimental results there is generally good agreement on the energy gap between empty and full surface states along the ΓJ direction on the surface. From these considerations, one can then conclude that the calculated electronic structures alone are not able to uniquely determine the nature of the transitions observed in EELS,[4,5] resulting in controversial interpretations of the available experimental optical data.[2,3,6,7] The evaluation of the surface dielectric response function for this system, and its analysis in terms of the associated electronic level structure, give further insights into this problem, as we discuss below.

In the present work, and in close connection with the general description of the optical properties of the C(111)-2×1 surface, we investigate in detail the origin of the electronic transitions related to the surface reconstruction. Our calculations employ a semiempirical tight-binding approach developed by Selloni, Marsella, and Del Sole,[12] and used to

study the optical properties of Si (111), (110), and (100),[12–15] and C(001) (Ref. 16) surfaces. Our tight-binding formalism is similar to the one used by Davidson and Pickett,[11] except that our extended orbital basis allows perhaps a better description of the conduction band due to its additional $s*$ orbital, and our level structure is in generally better agreement with experimental findings and other calculations.

Since we calculate the *surface* dielectric tensor, the results presented here can be compared directly with those measured using various optical spectroscopies. In particular, the differential reflectance and reflectance anisotropy spectroscopies provide accurate information about surface properties of metals[17] and semiconductors.[18] This is very important since several semiconductor surfaces show a metalliclike behavior due to the partially unoccupied surface state bands that hamper the use of electronic spectroscopies like ARPES, EELS, and scanning tunneling microscopy (STM). This indeed seems to be the case for the C(111)-2×1 surface, where a partly empty band has been found theoretically along one of the main directions on the surface,[8–11] while no direct experimental evidence is found in the literature for this metallic behavior. This behavior is in comparison with the Si and Ge (111)-2×1 reconstructed surfaces,[19,20] where the degeneracy of the surface states is broken by the buckling of the surface atoms, as the theoretical and experimental description of the surface states shows. Notice, furthermore, that the optical spectroscopies mentioned above have the advantage over other techniques of allowing *in situ* real-time measurements, which provide the invaluable opportunity of monitoring the chemical vapor deposition and molecular beam epitaxial growth,[21] as well as the dynamics of the chemisorption process.[22] The results presented here, then, not only provide answers to fundamental questions, but give important information for applications, which we expect will motivate future work in this direction.

In Sec. II, we present a brief discussion of the structural model of the surface and the methods used to calculate its electronic and optical properties. In Sec. III, we discuss our results and compare them with the available data in the literature. The results for the optical properties are presented in terms of the dielectric response of the surface, and the calculated reflectance anisotropy and EEL spectra.

II. MODELS AND METHOD OF CALCULATION

The diamond (111)-2×1 surface was modeled using a slab of 28 C layers with inversion symmetry, yielding a free reconstructed surface on each face of the slab. The thickness of the slab is large enough to decouple the surface states at the top and bottom surfaces of the slab. In Fig. 1, we show (a) the top view of the surface unit cell that contains two C atoms per layer, (b) a side view with only the six outermost layers of the slab, and (c) the irreducible surface Brillouin zone (SBZ). Periodic boundary conditions were employed parallel to the surface of the slab to effectively model a two-dimensional crystal system. The top (and bottom) layer of the slab, shown in Fig. 1 with larger dots, resembles the structure reported by Pandey.[23] In this Pandey chain model, the atoms of the top layer form a zigzag chain along one of the main directions on the surface plane (the x axis in Fig. 1).
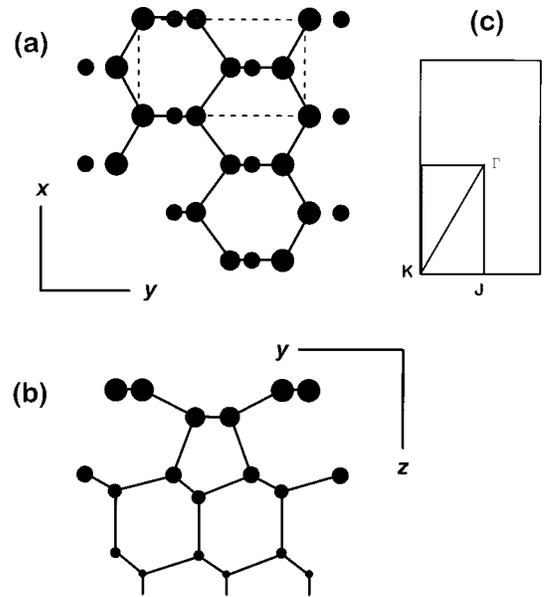

FIG. 1. Atomic model of the C(111)-2×1 surface. (a) Top view with the three uppermost layers; dashed line corresponds to the surface unit cell. (b) Side view with the six uppermost layers. The first-layer atoms forming Pandey-like chains are shown in larger dots. (c) Surface Brillouin zone is shown; shadowed area corresponds to its irreducible part. The main symmetry points are indicated.

The coordinates for the six outermost layers on each side were obtained by Alfonso *et al.*,[10] using a first-principles density functional based molecular dynamics technique due to Sankey and Niklewski.[24] (The remaining central layers have bulk geometry.) The method has been employed successfully in studying covalent systems such as silicon and carbon.[24–26] The relaxed C(111)-2×1 surface obtained with this method showed the zigzaglike chains with no buckling on the surface layer, and with CC bond lengths of about 1.44 Å. The results of Ref. 10 are in excellent agreement with previous self-consistent first-principles calculations,[9,27] where the authors find unbuckled surface chains with bond lengths equal to 1.47 and 1.44 Å, respectively. The reader is referred to Ref. 24 for a comprehensive description of this technique, and to Ref. 10 for a detailed discussion of its applicability to diamond surfaces. The use of the fully relaxed slab coordinates guarantees that the optical properties we calculate include all the subtle effects of surface-induced strain and appropriate geometry.

To calculate the optical properties of the system, we generate the electronic level structure of the slab using a well known parametrized tight-binding approach with an sp^3s* orbital basis.[28] This basis provides a good description of the conduction band of cubic materials. This approximation has been applied to calculate the optical properties of a variety of silicon surfaces,[12–15] and recently to the (001) surface of diamond,[16] yielding good results. The parameters for CC interactions are taken to be the same as those of Ref. 28 for the bulk, except for the on-site energy of the p_z orbitals of the surface atoms, E_p. This parameter is set to be 2.3 eV smaller than the corresponding bulk parameter. This change is as-

sumed to be the likely result of additional orbital confinement at the surface, and as we will see below, it yields a level structure more attuned to experiments and other theoretical calculations. Moreover, the scaling factor of all tight-binding parameters for this particular surface was taken as (r/r_0),[7] where r is the bond length of any two first-neighbor atoms and $r_0 = 1.56$ Å is the bond length in bulk diamond. These changes to the original bulk parameters provide an excellent description of the electronic structure, as compared to experimental measurements,[2,3,6,7] as we will show in Sec. III.

The optical properties of the surface region are determined by its dielectric function. The imaginary part of the average slab polarizability is related to the transition probability between slab eigenstates induced by an external radiation field.[29] Within a single-particle scheme, this relation is expressed by

$$\text{Im}\,\alpha_{\text{slab}}^{\alpha\alpha}(\omega) = \frac{\pi e^2}{m^2\omega^2 Ad}\sum_{\mathbf{k}}\sum_{v,c}|p_{vc}^{\alpha}(\mathbf{k})|^2$$

$$\times\,\delta(E_c(\mathbf{k})-E_v(\mathbf{k})-\hbar\omega), \qquad (1)$$

where $p_{vc}^{\alpha}(\mathbf{k})$ is the matrix element of the α component of the momentum operator between valence (v) and conduction (c) states at the point $\mathbf{k}$ of the SBZ, $2d$ is the slab thickness, m is the bare electronic mass, and A is the area of the surface unit cell. The real part of the average polarizability can be computed via the Kramers-Kronig relations. The surface dielectric tensor $\epsilon_{\text{surf}}^{\alpha\alpha}(\omega) = 1 + 4\pi\alpha_{\text{surf}}^{\alpha\alpha}(\omega)$ is then calculated from the average slab polarizability[30]

$$d\alpha_{\text{slab}}^{\alpha\alpha}(\omega) = d_{\text{surf}}\alpha_{\text{surf}}^{\alpha\alpha}(\omega) + [d-d_{\text{surf}}]\alpha_{\text{bulk}}(\omega)\delta_{\alpha\alpha}. \quad (2)$$

Here $\alpha_{\text{bulk}}(\omega) = [\epsilon_{\text{bulk}}(\omega)-1]/4\pi$ is the bulk polarizability, and d_{surf} is the depth of the surface region. Note that for cubic materials (C, Si, and Ge, for example) the bulk dielectric function is isotropic. The ''three-layer model'' of Drude[31] and McIntyre and Aspnes[32] adopted here is widely used in the analysis of optical data, and assumes that the system consists of three homogeneous regions, bulk, surface, and vacuum, and the dielectric response is treated accordingly.

The matrix elements of the momentum operator $p_{vc}^{\alpha}(\mathbf{k})$ of Eq. (1) were obtained in terms of the atomiclike orbital basis using the commutation relation between the Hamiltonian and position operator, $\mathbf{p} = i(m/\hbar)[H,\mathbf{r}]$. Taking advantage of the orthogonality and localization of the orbitals, only the intra-atomic dipole matrix elements are retained. Then, only two additional parameters to those of the tight-binding Hamiltonian were needed in order to reproduce the bulk dielectric function. These parameters are the so-called intra-atomic sp and s^*p dipoles, with best-fitted values of 0.18 Å and 0.7 Å, respectively. Notice that these calculations neglect in principle excitonic[35] and local field effects,[36] although the fitting parameter procedure compensates to some extent and yields very good agreement with bulk optical measurements. For a detailed description of the method the reader is referred to the pioneering work of Manghi et al.[30] and the review by Del Sole.[37]

In the above discussion, we have seen that the atomic structure of the surface region is intimately related to the dielectric response through its electronic structure, as given by Eq. (1). Experimentally, it is known that the surface dielectric function can be extracted by means of electronic and optical spectroscopies. Measurement of the reflectance anisotropy (RA) is one of these optical techniques, which consists of measuring the relative reflectance difference of two orthogonal light polarizations on the surface plane, x and y, for example. Although the sample penetration of light is in general a few hundred times larger than the depth of the surface layer, the contribution from the bulk region to the RA spectra is canceled since the bulk optical properties of cubic materials are isotropic. Correspondingly, this technique is extremely sensitive to surface features and electronic properties due to reconstructions or adsorption events.

Theoretically, the reflectivity is related to the dielectric function through the Fresnel formula,[38] which must, however, be modified due to the presence of the reconstructed surface region.[31–34] This correction yields the following expression for the differential reflectance spectrum when the light incidence is normal to the surface plane:[30]

$$\left(\frac{\Delta R}{R_0}\right)^{\alpha} = \frac{4\omega d}{c}\text{Im}\left[\frac{4\pi\alpha_{\text{slab}}^{\alpha\alpha}(\omega)}{\epsilon_{\text{bulk}}(\omega)-1}\right]. \qquad (3)$$

Here, α is one of the orthogonal directions on the surface plane, and $\Delta R = R - R_0$ is the difference between the actual reflection coefficient R and the reflectivity R_0 given by the Fresnel formula.

The second experimental technique in which we are interested is electron energy loss spectroscopy (EELS). Here, an electron beam of a given low energy and momentum is scattered by the sample. The electron beam induces polarizations in the surface region so that the electrons lose some of this energy before being scattered into the detector. The process can be described well in terms of a dipolar scattering theory,[39] and provides a suitable description of vibrational modes of surface atoms and molecules, as well as electron transitions in the surface region. In the present work, all of the electronic transitions in the surface region are due to the reconstruction of the surface and not to adsorbates, although the work could be generalized to include various adsorbate species as well.

The electron scattering probability $P(\mathbf{q}_{\parallel},\omega)$ for an electron that loses a quantum of energy $\hbar\omega$ and transfers a momentum $\hbar\mathbf{q}_{\parallel}$ in the direction of the surface plane is given by[39]

$$P(\mathbf{q}_{\parallel},\omega) = \frac{2}{(ea_0\pi)^2}\frac{1}{\cos\varphi_i}\frac{k'}{k}\frac{q_{\parallel}}{|q_{\parallel}^2+q_{\perp}^2|^2}\text{Im}g(\mathbf{q}_{\parallel},\omega),$$

$$\qquad (4)$$

where $\mathbf{k}$ and $\mathbf{k}'$ are the wave vectors of the incident and scattered electrons, φ_i is the angle of incidence, and $\hbar q_{\perp} = \hbar(k_z - k_{z'})$ is the momentum transfer in the direction perpendicular to the surface plane. The above relation holds when the energy loss and momentum transfer to the medium are small. Assuming that the scattering occurs in the yz plane, the loss function is defined by

$$\text{Im}g(q_y,\omega) = \text{Im}\left(\frac{-2}{1+\epsilon_{\text{eff}}(q_y,\omega)}\right), \qquad (5)$$
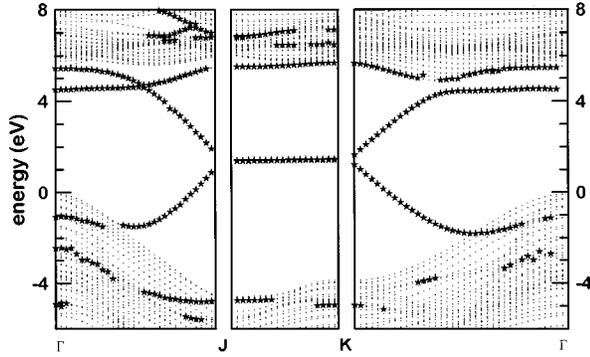
FIG. 2. Surface electronic structure along the main symmetry directions of the surface unit cell. Dots correspond to the projected bulk states, while stars represent surface states. Resonance states embedded in projected bulk bands are also represented by stars.

where $\epsilon_{\text{eff}}(q_y,\omega)$ is the nonlocal effective dielectric function of the system. In the limit $q_z d_{\text{surf}} \ll 1$, when the momentum transfer to the medium in the perpendicular direction to the surface plane is small, this effective dielectric function becomes

$$\epsilon_{\text{eff}}(q_y,\omega) \approx \epsilon_{\text{bulk}}(\omega) + q_y d_{\text{surf}}[\epsilon_{\text{surf}}^{yy}(\omega) - \epsilon_{\text{bulk}}^2(\omega)/\epsilon_{\text{surf}}^{zz}(\omega)]. \tag{6}$$

This theory has been applied successfully to explain the experimental EELS spectra of the 2×1 and 7×7 reconstructions of the Si(111) surface.[15,40]

In the following section we use our calculated surface dielectric function to explain the main features of RA and EELS spectra of the C(111)-2×1 surface.

III. RESULTS AND DISCUSSION

A. Surface band structure

The electronic band structure of the C(111)-2×1 surface is presented in Fig. 2. The electronic structure is shown along the main symmetry directions of the irreducible SBZ, from Γ to J (x direction), from J to K (y direction), and from K to Γ (diagonal). The states associated with the surface reconstruction are represented by stars,[41] while dots correspond to the projected bulk states. The top of the bulk valence band is set at 0 eV, and the calculated Fermi level (E_f) is at about 1.5 eV (not indicated in Fig. 2), and coincident with the nearly-degenerate and flat dispersion states along JK. The calculated E_f is in excellent agreement with the reported experimental value of 1.5 ± 0.2 eV.[2,3,6,7] In fact, the calculated results presented here are in excellent general agreement with the experimental findings measured along the ΓJ and $K\Gamma$ directions[2,3,6,7] and also compare well in all the main directions with those calculated previously using first-principles[8–10] and parametrized tight-binding[11] approaches.

The calculated surface band structure of Fig. 2 shows a large gap of about 5.5 eV between the occupied and unoccupied surface states at the Γ point. The occupied surface states lying within the bulk valence band show a dispersion of $\sim$ 2.4 eV along the ΓJ direction (the Pandey chain axis direction), and have mainly a p_z character. The behavior of

these states is similar to one observed experimentally by Himpsel and co-workers[2] and Pate and co-workers,[3] where a nearly flat filled surface band is found from Γ to about 0.5 ΓJ where there is a minimum, and then rapidly disperses upward while approaching the J point. A similar behavior is found for these surface states along the ΓK direction. Above the Fermi level there are two bands of unoccupied states near 4.5 and 5.5 eV at the Γ point. These states have a strong s and p_z component corresponding to the dangling bonds of the surface chain atoms and the backbonds with the second- and third-layer atoms. The states at 4.5 eV show a nearly flat band in the first half of the ΓJ and ΓK directions; at about the halfway point in both directions the band has a maximum and then rapidly disperses downward approaching the J and K points. In the direction perpendicular to the chain, JK, these empty surface states and the occupied surface band become nearly degenerate and show little dispersion, less than 0.1 eV. Notice that these two states cross the Fermi level halfway through the JK direction. The striking difference in dispersion of the surface bands along the two main directions is a reflection of the Pandey-like chains formed on the surface. The chains along the ΓJ (or x) direction allow for electronic motion that could be explained in analogy to the nearly-free-like well known case (although the dispersion is not parabolic here), while the nearly vanishing overlap between the chains along the JK (or y) direction yields nearly flat surface bands and reduces electronic hopping across zigzag chains.

Near $\sim$5.5 eV at the Γ point begins a band of unoccupied surface states mainly due to the surface dangling bonds, and partly to second-layer backbonds, corresponding approximately to those calculated by Vanderbilt and Louie[8] and Alfonso and co-workers,[10] and likely to be those observed by Kubiak and Kolasinski.[7] These states show a dispersion of about 1 eV with a minimum at about halfway along the ΓJ direction, where they anticross the surface band associated with the backbond states described above, and produce a hardly noticeable splitting at the crossing. On the other hand, these states show less dispersion ($\sim$0.5 eV) along the ΓK direction and never cross the empty surface dangling bonds band. These states have also been observed experimentally by Kubiak and Kolasinski[7] with a weak intensity at an energy of about 5.8 eV from the top of the valence band, for both the ΓJ and ΓK directions. Along the JK direction these states are more localized in the second and third layers, with a strong back-antibonding character. Finally, some localized resonancelike occupied states are also found at -2.5 eV and at -4.8 eV near the Γ point (shown as stars within the valence band in Fig. 2). The former states are mainly due to the subsurface chains with a strong p_x component, and the latter have first- and second-layer backbond characteristics. The states at -2.5 eV are similar to those reported by Vanderbilt and Louie.[8]

Experimental photoemission results show occupied[2,3] and unoccupied[6,7] surface states with a gap of nearly 5.1 eV at the Γ point. The Fermi level is reported at about 1.5 eV above the top of the valence band, similar to our findings, while the dispersion and location of the observed surface states are also in very good agreement with those calculated here. (On the other hand, only the dispersion of the observed surface states is in good agreement with those reported by
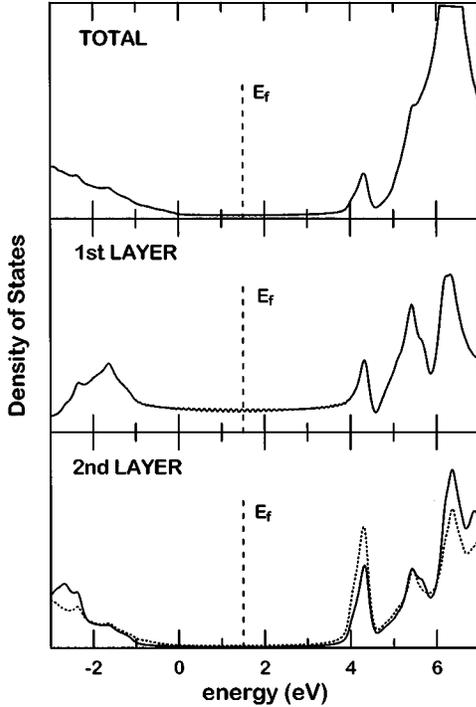
FIG. 3. Calculated density of states for (a) total, (b) projected on first layer, and (c) projected on second layer (solid) and third layer (dotted line). Different vertical scales used in each panel.

Vanderbilt and Louie[8] and Davidson and Pickett.[11]) Moreover, since these surface states are detectable only for p polarization, they show a strong s and p_z character, in agreement with our results. A resonance unoccupied state has also been observed at about 6 eV from the top of the valence band at the Γ point.[7] This resonance state is much weaker than the surface states lying in the fundamental gap, and it has not been possible to fully investigate its orbital character, although it could be the higher-energy surface state we find.

While the calculated surface bands in Fig. 2 compare well with the experimental results,[2,3,6,7] notice that the calculated LDA (Ref. 8) and tight-binding[11] surface bands are rigidly shifted with respect to the top of the valence band by +1 and +2 eV, respectively. The discrepancies among the different approaches could perhaps be partly attributed to many-body effects. For example, when the exchange correlation effects are considered, the surface band is shifted towards the top of the projected bulk valence band.[8,9] Moreover, when dynamical effects are taken into account within the GW approximation, the surface band moves into the projected bulk valence band in the vicinity of the Γ point,[42] also in agreement with experimental results.[2,3] However, there could be other sources of error when we compare directly with experimental results, including the precise experimental location of the Fermi level, as pointed out before.[8]

The total electronic density of states (DOS) of the slab, and the projected density of states of the first two layers are shown in Fig. 3. The DOS was calculated taking an average over 4900 points distributed homogeneously in the irreducible SBZ. We observe within the fundamental bulk gap, between 0 and 5.5 eV, a nonzero density of states coming mainly from the dangling bonds associated with first-layer

atoms. This continuum of surface states is responsible for the metalliclike behavior of the surface around the Fermi level, as we will discuss in detail in the next section. Notice that the DOS from 0 to 4 eV is nearly a constant, as expected for a two-dimensional (2D) free-electron system. From Fig. 3 is clear that the peak at about 4.5 eV with a strong p_z component has its origin in the dangling bond and the first- and second-layer backbonds. The resonance states at about −2.5 and 5.5 eV are associated with the second-layer chains and the backbonds between the first-layer and second-layer atoms, respectively. The pronounced peaks of the projected DOS in the first layer, at about −1.5 and 4.5 eV, are due to the lack of dispersion of the surface bands on the first half of the ΓJ and ΓK directions of the SBZ (see Fig. 2). Here, we observe that the states in the bulk gap are mainly localized in the first two layers, as one would expect, with decreasing intensity into the slab.

Finally, before addressing the optical consequences of this level structure, we should comment on our choice of parameters. The excellent agreement with experiments and *ab initio* electronic calculations has been greatly enhanced by our use of the different E_{p_z} parameter for the surface atoms, as mentioned above, as well as to the fully relaxed atomic positions for the reconstructed surface of Ref. 10. Indeed, use of the *bulk* E_{p_z} parameters for all surface atoms yields a level structure (not shown) very similar to that of Davidson and Pickett.[11] In that case, we obtain $E_f \approx 3.5$ eV above the valence-band top, while the filled surface dangling bond state remains ≈ 2.7 eV below E_f (but now *above* the valence band). Similarly, the gap between surface state and conduction-band bottom along the JK direction is only ≈ 2.5 eV, rather than the 4 eV gap shown in Fig. 2. This full set of results validates the choice of the physical parameter E_{p_z} at the surface. Although a detailed fit to the experimental results was not performed, it is clear (as one would expect on general physical grounds) that the orbital localization at the surface affects the diagonal tight-binding parameters. A full *ab initio* determination of the various optical parameters, both in the bulk and near the surface, together with the fully relaxed level structure, will be obviously desirable. We are currently carrying out such a project and our results will be presented elsewhere.

B. Surface dielectric properties

The imaginary part of the average polarizability of the slab, Eq. (1), was calculated using 4900 points distributed homogeneously on the irreducible SBZ. The large number of points needed is due to the small (large) size of the surface unit cell in real (reciprocal) space and to the large sections of the SBZ with flat joint density of states. The average over this large number of points is necessary to give full and reliable convergence of the optical properties for this particular surface. Electron transitions up to 20 eV were taken into account, so that after the Kramers-Kronig transform the calculated real part is accurate up to about 10 eV.

In Fig. 4, we present the real and imaginary parts of the surface dielectric tensor $\epsilon_{surf}(\omega)$ calculated from Eq. (2). The thickness of the surface region used was $d_{surf} = 2.5$ Å, which approximately corresponds to two monolayers (other choices of d_{surf} do not change qualitatively our results for energies in
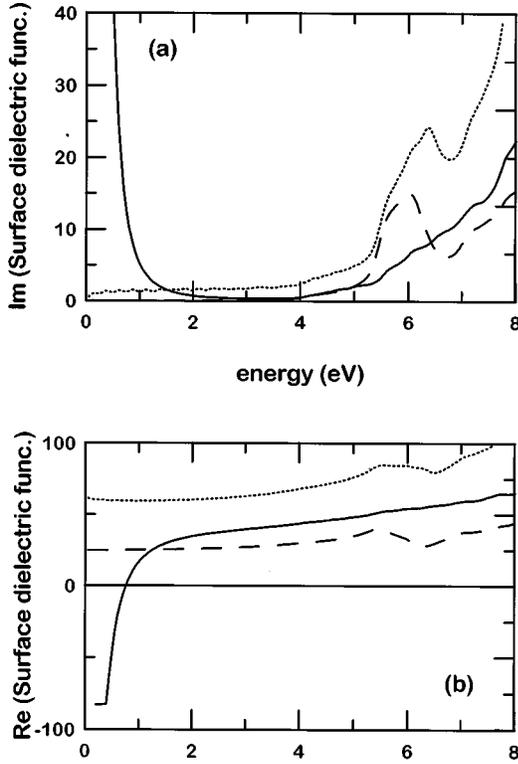
FIG. 4. The (a) imaginary part and (b) real part of the *surface* dielectric response. Solid lines correspond to light polarized along the chains (*x* axis), ϵ_{surf}^{xx}, while dotted lines correspond to light polarized perpendicular to the chain (*y* axis), ϵ_{surf}^{yy}. The dashed line corresponds to light polarized perpendicular to the surface, ϵ_{surf}^{zz}.

FIG. 5. Total differential reflectance spectrum divided into its *S-S*, *S-B*, *B-B*, and *B-S* components. Solid lines in bottom four panels correspond to light polarized along the chain (*x* axis), while the dotted lines correspond to light polarized perpendicular to the chains (*y* axis).

the bulk gap). The response for light polarized along the chains (*x* axis, ϵ_{surf}^{xx}) corresponds to the solid lines, while for light polarized in the *y* direction (ϵ_{surf}^{yy}) it is shown by dotted lines, and the dashed lines correspond to the direction perpendicular to the surface plane (ϵ_{surf}^{zz}). The imaginary part of $\epsilon_{surf}(\omega)$ along *x* shows a strong peak at about 0.1 eV that is 100 times more intense than the rest of the structure shown in Fig. 4. This peak at low energy is a reflection of the metalliclike character of the surface along the chains. Then, from 2 to 5.5 eV, the dielectric function is nearly constant up to the point when electron transitions between bulk states become important.

The following discussion about the origin of the main electron transitions of the surface dielectric function can be followed clearly in the lower four panels of Fig. 5, where the reflectance anisotropy spectrum has been decomposed into the different contributions *S-S, S-B, B-B,* and *B-S*. For light polarized in both directions, *x* and *y*, the dielectric response is dominated by transitions among surface states (*S-S*) up to ~ 4 eV. From about 4 eV the contribution of the transitions from surface to bulk states (*S-B*) and from bulk to surface states (*B-S*) becomes important. Note that the gap between the partly occupied flat band of surface states along the *JK* direction on the SBZ (see Fig. 2) and the bottom of the bulk conduction band is about 4 eV. Likewise for the gap between valence bulk states and the unoccupied surface band at the Γ point. The high density of surface states above and below
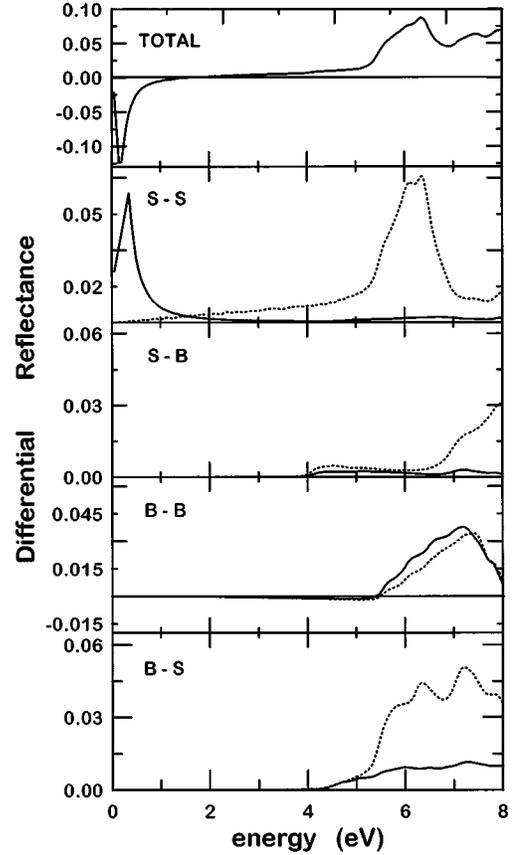
the Fermi level along Γ*J* results in large *S-B* and *B-S* contributions to the Im$\epsilon_{surf}(\omega)$ along the *y* direction (perpendicular to the chains; shown dotted in Fig. 4). Only for this perpendicular direction to the chains does the Im$\epsilon_{surf}(\omega)$ show an intense peak centered at about 6 eV due to *S-S* transitions. The transitions between bulk states (*B-B*) become important from about 5.5 eV onwards, where the response to *x* and *y* polarizations is very similar, as one expects for cubic semiconductors (notice also the scale change as the traces are much weaker). For light polarized perpendicular to the surface plane (*z* direction), the ϵ_{surf}^{zz} shows also a peak around 6 eV mainly due to the first- and second-layer backbond states (figure not shown).

In the rest of this section we will discuss the reflectance anisotropy and electron energy loss spectra obtained using the calculated surface dielectric function.

1. Reflectance anisotropy

In Fig. 5, the top panel shows the differential reflectance anisotropy spectra for light at normal incidence, $(\Delta R/R_0)^y - (\Delta R/R_0)^x$, calculated according Eq. (3), and labeled ''TOTAL.'' This has been decomposed into its different contributions, where the response to light polarized along *x* (chain axis) corresponds to the solid line, while the dotted

line corresponds to light polarized along y (perpendicular to the chain). From the figure, it is clear that the spectrum shows a large surface anisotropic optical response in a large range of photon energies. While for x-polarized light the spectrum shows mainly one peak at low energies, the y-polarization spectrum shows a rich structure for all energies inside the bulk optical gap.

The intense peak at ~ 0.1 eV corresponding to x-polarized light is totally determined by transitions between surface states. As we have explained above, this peak is related to the metalliclike behavior of the surface along the chain axis. At about 6 eV there are also some S-S transitions of weaker intensity for x polarization, and associated with the resonance states in the conduction band. The rest of the x-polarized spectrum shows a very small contribution from S-B and B-S transitions, compared to the response for y-polarized light. In fact, the response to light polarized perpendicular to the chain axis (y direction) shows much more structure in a larger energy region within the bulk optical gap. Up to ~ 4 eV the spectrum is only dominated by S-S transitions. At 4 eV the contribution from S-B and B-S transitions starts and is reflected in the total differential spectrum by a shoulder. As mentioned above, 4 eV corresponds to the gap between the flat band surface states around E_f along JK and the bottom of the conduction band, as well as to the energy difference between valence bulk states and the unoccupied surface band beginning at 4.5 eV at the Γ point. Then the intensity enhancement of the S-B contribution starting from $\sim$ 6.5 eV corresponds to an increase of the density of the conduction-band states. In all cases, the B-B contributions to the total differential reflectance spectra in this range are insignificant, since both polarizations yield nearly identical contributions.

It is important to notice that this kind of *deconvolution* of the spectrum helps one gain useful insights into the nature of the various transitions. As we have pointed out, the S-B contribution starts at some determined energy (≈ 4 eV), as this gap is related to the conduction-band and surface states located around E_f. This part of the spectrum gives then unambiguous information on the position of the Fermi level with respect to the bulk band structure, and therefore the energy at which the filled surface states are. Notice that one important advantage of this optical spectroscopy is the high precision in measuring the energy at which the electronic transitions occur. The present results could be important for a future comparison with reflectance anisotropy measurements in order to better determine the electronic structure associated with this particular reconstruction of the surface. We hope this motivates additional experiments.

2. EELS

The calculated scattering probability of an EELS experiment, using Eq. (4), is shown in Fig. 6. The primary energy of the electron beam was taken equal to 80 eV, with a normal incidence geometry. The spectrum corresponding to an electron beam polarized along the chain (solid line) is very different at low energies (less than 1 eV) than the results for a polarization perpendicular to the chains (dotted line). The intensity of the x-polarized reflected beam is a few thousand times larger that the beam for y-direction polarization. At higher energies, from about 4 eV onwards, the two spectra
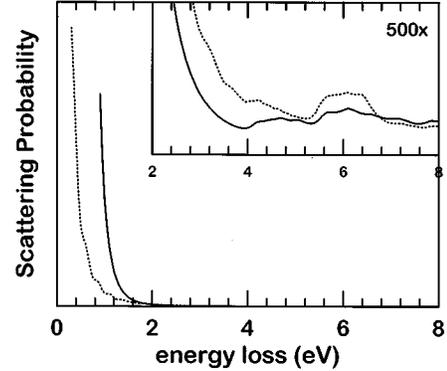

FIG. 6. Scattering probability function for electron energy loss, Eq. (4). Solid lines correspond to light polarized along the chain (x axis), while dotted lines correspond to light polarized perpendicular to the chains (y axis). The inset has been amplified 500 times.

show similar amplitude and behavior. The inset shows the scattering probability for energy loss from 2 to 8 eV, where the intensity has been augmented 500 times. Here, a feature starts at about 4 eV. As we discussed above, these structures are related to the contribution to the surface dielectric response from S-B and B-S transitions, while the broad peak at about 6 eV is produced by S-S transitions. Notice that the high-energy-loss features are strongly reduced by the decaying prefactor $1/q_{\parallel}$ appearing in the definition of P, Eq. (4).

The EELS experiments reported by Pepper[4] showed a broad structure centered near 2.1 eV (and with width of about 1.7 eV). The primary energy of the normal incident electron beam was $E_0 = 80$ eV. The main spectrum reported by Pepper was obtained by subtracting the spectra measured for the clean and hydrogenated surfaces, in order to reduce the effects of a strong elastic peak and to enhance the signal due to the reconstruction. The spectra of the clean and hydrogenated surfaces were obtained from an average over the SBZ. In the difference spectrum a minimum gap of about 1 eV was observed and identified with the effective gap between surface states at the point J. The energy resolution of the system is estimated at 0.63 eV, from the width of the elastic peak remnant. Since the energy resolution is not optimal in this experiment, it is difficult to make a direct comparison with theoretical calculations and other experiments. Moreover, the energy loss measured by this kind of spectroscopy is generally smaller than the energy difference between occupied and unoccupied states of the system in its ground state. Therefore it is possible that the observed broad feature at 2.1 eV is related to the S-S transitions integrated over the SBZ, and expected to have an enhanced joint DOS at ≈ 6 eV. The overall resulting feature would perhaps be a combination of excitonic downshift and the high-energy ($1/q_{\parallel}$) suppression factor. It is clear, however, that a better-resolution and more detailed EELS study on this system will be highly desirable. We will be glad to provide details of our electronic structure and surface dielectric function results to interested experimental groups.

IV. CONCLUSIONS

We have investigated the optical response of the C(111)-2 $\times 1$ surface based on an sp^3s^* parametrized tight-binding

approach. The dielectric function of the surface region was calculated and a large anisotropy was found. This anisotropy of the optical response is a direct consequence of the surface reconstruction. The dielectric response of the surface was analyzed in terms of the *S-S*, *S-B*, *B-B*, and *B-S* transitions, and important features corresponding to each type of transition were found. The reflectance anisotropy and electron energy loss spectra were calculated in order to provide direct comparison with experiments. We can conclude that these optical spectroscopies, combined with theoretical studies, can help one elucidate the controversial surface electronic structure, and therefore the structural and electronic level reconstruction, of this important surface.

ACKNOWLEDGMENTS

[1] See, for example, F.G. Celii and J.E. Butler, Annu. Rev. Phys. Chem. **42**, 643 (1991).

[2] F.J. Himpsel, D.E. Eastman, P. Heidmann, and J.F. Van der Veen, Phys. Rev. B **24**, 7270 (1981).

[3] B.B. Pate, Surf. Sci. **165**, 83 (1986); B.B. Pate, J. Woicik, J. Hwang, and J. Wu, in *Science and Technology of New Diamond*, edited by S. Saito, O. Fukunaga, and M. Yoshikawa (Terra Scientific Publishing Company, 1990), p. 345.

[4] S.V. Pepper, J. Vac. Sci. Technol. **20**, 213 (1982); Surf. Sci. **123**, 47 (1982).

[5] P.G. Lurie and J.M. Wilson, Surf. Sci. **65**, 476 (1977).

[6] J.F. Morar, F.J. Himpsel, G. Hollinger, J.L. Jordon, G. Hughes, and F.R. McFeely, Phys. Rev. B **33**, 1346 (1986).

[7] G.D. Kubiak and K.W. Kolasinski, Phys. Rev. B **39**, 1381 (1989).

[8] D. Vanderbilt and S.G. Louie, Phys. Rev. B **30**, 6118 (1984).

[9] S. Iarlori, G. Galli, F. Gygi, M. Parrinello, and E. Tosatti, Phys. Rev. Lett. **69**, 2947 (1992).

[10] D.R. Alfonso, D.A. Drabold, and S.E. Ulloa, Phys. Rev. B **51**, 14 669 (1995).

[11] B.N. Davidson and W.E. Pickett, Phys. Rev. B **49**, 11 253 (1994).

[12] A. Selloni, P. Marsella, and R. Del Sole, Phys. Rev. B **33**, 8885 (1986).

[13] R. Del Sole, W.L. Mochán, and R.G. Barrera, Phys. Rev. B **43**, 2136 (1991).

[14] A. I. Shkrebtii and R. Del Sole, Phys. Rev. Lett. **70**, 2645 (1993).

[15] C. Noguez, A.I. Shkrebtii, and R. Del Sole, Surf. Sci. **318**, 342 (1994); **331-333**, 1349 (1995).

[16] V.I. Gavrilenko and A.I. Shkrebtii, Surf. Sci. **324**, 226 (1995).

[17] Y. Borensztein, W.L. Mochán, J. Tarriba, R.G. Barrera, and A. Tadjeddine, Phys. Rev. Lett. **71**, 2334 (1993); Ph. Hofmann, K.C. Rose, V. Fernandez, A.M. Bradshaw, and W. Richter, *ibid.* **75**, 2039 (1995).

[18] P. Chiaradia *et al.*, Phys. Rev. Lett. **52**, 1145 (1983); T. Yasuda, L. Matense, U. Rossow, and D.E. Aspnes, *ibid.* **74**, 3431 (1995).

[19] R.I. Uhrberg, G.V. Hansson, J.M. Nicholls, and S.A. Flodström, Phys. Rev. Lett. **48**, 1032 (1982); J.E. Northrup and M.L. Cohen, *ibid.* **49**, 1349 (1982); F. Ancilotto, W. Andreoni, A. Selloni, R. Car, and M. Parrinello, *ibid.* **65**, 3148 (1990).

[20] J.M. Nicholls, G.V. Hansson, R.I. Uhrberg, and S.A. Flodström, Phys. Rev. B **27**, 2594 (1983); J.E. Northrup and M.L. Cohen, *ibid.* **27**, 6553 (1983); N. Takeuchi, A. Selloni, A.I. Shkrebtii, and E. Tosatti, *ibid.* **44**, 13 611 (1991).

[21] D.E. Aspnes, J.P. Harbison, A.A. Studna, and L.T. Florez, Phys. Rev. Lett. **59**, 1687 (1987); A.R. Turner, M.E. Pemble, J.M. Fernandez, B.A. Joyce, J. Zhang, and A.G. Taylor, *ibid.* **74**, 3213 (1995).

[22] M. Roy and Y. Borensztein, Surf. Sci. **331−333**, 453 (1995).

[23] K.C. Pandey, Phys. Rev. B **25**, 4338 (1982).

[24] O.F. Sankey and D.J. Niklewski, Phys. Rev. B **40**, 3979 (1989).

[25] G.B. Adams, O.F. Sankey, M. O'Keefe, J.B. Page, and D.A. Drabold, Science **256**, 1792 (1992).

[26] D.A. Drabold, P.A. Fedders, S. Klemm, and O.F. Sankey, Phys. Rev Lett. **67**, 2179 (1991); D.A. Drabold, R. Wang, S. Klemm, and O.F. Sankey, Phys. Rev. B **43**, 5132 (1991).

[27] R. Stumpf and P.M. Marcus, Phys. Rev. B **47**, 16 016 (1993).

[28] P. Vogl, H. P. Hjalmarson, and J. D. Dow, J. Phys. Chem. Solids **44**, 365 (1983).

[29] F. Bassani and G. Pastori Parravicini, *Electronic States and Optical Transitions in Solids* (Pergamon Press, New York, 1975).

[30] F. Manghi, R. Del Sole, A. Selloni, and E. Molinari, Phys. Rev. B **41**, 9935 (1990).

[31] P. Drude *The Theory of Optics* (Dover, New York, 1959).

[32] J.D.E. McIntyre and D.E. Aspnes, Surf. Sci. **24**, 417 (1971).

[33] A.G. Bagchi, R.G. Barrera, and A.K. Rajagopal, Phys. Rev. B **20**, 4824 (1979); W.L. Mochán, R. Fuchs, and R.G. Barrera, *ibid.* **27**, 771 (1983).

[34] W.L. Schaich and W. Chen, Phys. Rev. B **39**, 10 714 (1989), and references therein.

[35] R. Del Sole and E. Fiorino, Phys. Rev. B **29**, 4631 (1984).

[36] W.L. Mochán and R.G. Barrera, Phys. Rev. Lett. **55**, 1192 (1985); **56**, 2221 (1986).

[37] R. Del Sole, in *Electromagnetic Waves: Recent Developments in Research, Vol. 2: Photonic Probes of Surfaces*, edited by P. Halevi (Elsevier, Amsterdam, 1995), p. 131.

[38] J.D. Jackson, *Classical Electrodynamics*, 2nd ed. (Wiley, New York, 1975).

[39] H. Ibach and D.L. Mills, *Electron Energy Loss Spectroscopy and Surface Vibrations* (Academic Press, New York, 1982).

[40] A. Selloni and R. Del Sole, Surf. Sci. **168**, 35 (1986).

[41] The surface and resonance states are labeled using an empirical parameter δ_0. This parameter is chosen so that the states have a larger probability ($> \delta_0$) of being localized on/around the surface region than the projected bulk states ($< \delta_0$).

[42] C. Kress, M. Fiedler, and F. Bechstedt, Europhys. Lett. **28**, 433 (1994).